

# EXIT-Chart Optimised Short Block Codes for Iterative Joint Source and Channel Decoding in H.264 Video Telephony

Nasruminallah and L. Hanzo

School of ECS, University of Southampton, SO17 1BJ, UK.

<http://www-mobile.ecs.soton.ac.uk>,

Email: {1h}@ecs.soton.ac.uk

**Abstract**— In this paper we propose a family of Short Block Codes (SBCs) designed for guaranteed convergence in soft-bit assisted iterative joint source and channel decoding, which facilitate improved iterative soft-bit source decoding (SBSD) and channel decoding. Data-Partitioned (DP) H.264 source coded video is used to evaluate the performance of our system using SBC assisted SBSD in conjunction with Recursive Systematic Convolutional Codes (RSC) for transmission over correlated narrowband Rayleigh fading channels. The effect of different SBC schemes having diverse minimum Hamming distances ( $d_{H,min}$ ) and code rates on the attainable system performance is demonstrated, when using iterative SBSD and channel decoding, while keeping the overall bit-rate budget constant by appropriately partitioning the total available bit rate budget between the source and channel codecs to improve the overall BER performance and to enhance the objective video quality expressed in terms of Peak Signal-to-Noise Ratio (PSNR)<sup>1</sup>. EXIT Charts were used for analysing the attainable system performance. Explicitly, our experimental results show that the proposed error protection scheme using rate- $\frac{1}{3}$  SBCs having  $d_{H,min} = 6$  outperforms the identical-rate SBCs having  $d_{H,min} = 3$  by about 2.25 dB at the PSNR degradation point of 1 dB. Additionally, an  $E_b/N_0$  gain of 9 dB was achieved compared to the rate- $\frac{5}{6}$  SBC having  $d_{H,min} = 2$  and an identical overall code-rate. Furthermore, an  $E_b/N_0$  gain of 25 dB is attained at the PSNR degradation point of 1 dB, while using iterative soft-bit source and channel decoding with the aid of rate- $\frac{1}{3}$  SBCs relative to the identical-rate benchmark.

## I. MOTIVATION AND BACKGROUND

Reliable transmission of multimedia source coded streams over diverse wireless communication networks, constitutes a challenging research topic [1, 2]. Since the early days of wireless video communications [3–6] substantial further advances have been made both in the field of proprietary and standard-based solutions [7, 8]. Furthermore, the joint optimisation of different functions such as joint source and channel decoding (JSCD) gained considerable attention. The family of JSCD schemes often relies on exploiting the residual redundancy in the source-coded bit-stream. Finscheidt and Vary [9, 10] proposed SBSD to exploit the natural residual redundancy of the source-coded bit-stream for improving the convergence of Iterative Source-Channel Decoding (ISCD) [11, 12]. However, only moderate residual redundancy is left in the source coded

bit-stream, when using advanced state-of-the-art coding techniques. Therefore we propose to deliberately impose additional redundancy on the source coded bit-stream with the aid of the novel class of SBCs proposed. In our experimental setup the H.264/AVC video codec [13] is used to encode the input video sequence and to generate the source coded bitstream. The H.264/AVC codec employs heterogeneous Variable Length Coding (VLC) and predictive coding techniques to achieve a high compression efficiency, which makes the compressed bit-stream susceptible to transmission errors [1]. A single bit error in the coded stream may corrupt the decoding of numerous future codewords. Moreover, due to predictive coding the effects of channel errors may affect the neighboring video blocks due to error propagation. Therefore the transmission of compressed video over wireless systems is a challenging task. Various error resilient schemes have been proposed in [1], in order to alleviate these problems, but the price paid is a potential reduction of the achievable compression efficiency and increase in computational complexity. An iterative joint source-channel decoding procedure inspired by the concept of serial concatenated codes was presented in [14]. A symbol-based soft-input a posteriori probability (APP) decoder was presented in [15], where the residual redundancy was exploited for improved error protection. Instead of the traditional serial concatenation of the classic Variable Length Codes (VLC) with a channel code, a parallel concatenated coding scheme was presented in [16], where the VLCs were combined with a turbo code. On the other hand, a novel irregular variable length coding (IrVLC) scheme designed for near-capacity joint source and channel coding was proposed in [17]. Likewise, [18] advocated the employment of state-of-the-art High-Speed Packet Access (HSPA)-style [19] burst-by-burst adaptive transceivers for interactive cellular and cordless video telephony, which are capable of accommodating the time-variant channel quality fluctuation of wireless channels. An iterative source and channel decoding aided Irregular Convolutional Coded (IRCC) videophone scheme using Reversible Variable-Length Codes (RVLC) and the Maximum A-Posteriori (MAP) [20] detection algorithm was proposed in [21]. The performance analysis of soft bit assisted iterative joint source and channel decoding was presented in [22], where Differential Space-Time Spreading (DSTS) aided Sphere Packing (SP) modulation was invoked which dispensed with channel estimation and provided both spatio-temporal diversity as well as a multi-user support. Furthermore, a joint source-channel decoding method based

<sup>1</sup>PSNR is the most widely used and simple form of objective video quality measure, which represents the ratio of the peak to peak signal to the root mean squared noise [1].

Copyright (c) 2008 IEEE. Personal use of this material is permitted. However, permission to use this material for any other purposes must be obtained from the IEEE by sending a request to [pubs-permissions@ieee.org](mailto:pubs-permissions@ieee.org).

on the MAP algorithm was proposed by Wang and Yu [23]. Instead of the well known convolutional coded ISCD, an ISCD based on two serial concatenated short block codes was proposed by Clevorn *et al.* [24]. In the above-mentioned scheme a (6, 3) outer block code served as a redundant index assignment, while a *rate-1* block code was used as inner code. Similarly, Thobaben [25] provided the performance analysis of a rate  $R = \frac{4}{5}$  single parity check code used for protecting the quantised source symbols relative to specifically designed VLCs. Joint source channel coding schemes employing a rate  $R = \frac{4}{5}$  linear block code for mapping the quantised source symbols to a binary representation were combined with an inner irregular channel encoder in [26]. An optimised bit rate allocation scheme using a rate  $r^* = 1^2$  inner channel encoder along with  $k = 3$  to  $k^* = 6$  source mapping was proposed in [27], and its performance was evaluated relative to conventional ISCD using a rate  $r = \frac{1}{2}$  recursive non-systematic convolutional (RNSC) inner code. The Turbo DeCodulation scheme presented in [28, 29] consisted of two iterative loops. The inner loop was constituted by the two components of Bit-Interleaved Coded Modulation using Iterative Decoding (BICM-ID) and the outer loop by the Iterative Source-Channel Decoding (ISCD) scheme. By contrast, in [30] a short block code based redundant index assignment and multi-dimensional mapping were used to artificially introduce redundancy and a single iterative loop was employed. Similarly, Clevorn *et al.* [31] presented a new design and optimisation guidelines for the ISCD's performance improvement using the concept of redundant index assignment with specific generator matrices.

In contrast to this background, where specific mapping examples were provided for iterative source and channel coding, we present powerful yet low-complexity algorithms for SBCs, which can be used to generate SBCs for a variety of mapping rates associated with diverse  $d_{H,min}$  values that are applicable to wide-ranging multimedia services. Additionally, instead of modelling the sources with the aid of their correlation, the practically achievable interactive video performance trends are quantified when using state-of-the-art video coding techniques, such as H.264/AVC. More explicitly, instead of assuming a specific source-correlation model, we based our system design examples on the simulation of the actual H.264/AVC source coded bit-stream. The SBC-aided SBSD scheme was utilised for protecting the H.264 coded bit-stream using Recursive Systematic Convolution (RSC) codes [20]. The SBC coding scheme was incorporated by carefully partitioning the total available bit-rate budget between the source and channel codecs, which results in an improved performance when ISCD is employed. Explicitly, an  $E_b/N_0$  gain of 25 dB is attained using ISCD, when employing a rate- $\frac{1}{3}$  SBC scheme in comparison to a realistic identical-rate benchmarker dispensing with the SBC scheme.

The rest of the paper is organised as follows. In Section II we portray our system model along with an overview of the H.264 encoded bit-stream and SBSD. An overview of

ISCD is provided in Section III along with our proposed SBC coding algorithms, accompanied by a design example. Section IV provides the EXIT chart analysis of our proposed system model, while the performance of the proposed system is characterised with the aid of our simulation results in Section V. Finally we offer our conclusions in Section VI.

## II. SYSTEM OVERVIEW

### A. H.264 Coded Stream Structure

The H.264/AVC codec's structure is notionally divided into the Video Coding Layer (VCL) and the Network Abstraction Layer (NAL) [32]. The hybrid video coding functions designed for improved coding efficiency are part of the VCL, while the NAL is designed for improved network adaptation and is responsible for the reliable transport of the resultant bit-stream generated by VCL over a wide range of transport layer protocols. The H.264/AVC generates a number of video-frame slices, which are formed by an integer number of consecutive Macro Blocks (MBs) of a picture. The number of MBs per slice may vary from a single one to all MBs of a picture in a given slice. Error resilient Data Partitioning (DP) [33] has been incorporated in the H.264/AVC codec in order to mitigate the effects of channel errors. In the H.264/AVC codec DP results in three different types of streams per slice, which are referred to as Type A, B and C partitions, each containing specific sets of coding parameters having different levels of importance. Additionally, the H.264 coded stream contains information related to the Group of Pictures (GOP) sequence and a so-called picture parameter set containing information related to all the slices of a single picture. All these different syntax elements are contained in Network Abstraction Layer Units (NALUs), consisting of 1-byte header and a payload of a variable number of bytes containing the coded symbols of the corresponding H.264 syntax element. The type of data contained by the NALU is identified by the 5-bit NALU type field contained in the NALU header.

### B. System Model

The schematic of our proposed videophone arrangement used as our design example for quantifying the performance of various SBC schemes is shown in Figure 1. At the transmitter side the video sequence is compressed using the H.264 video codec and the video source bit-stream  $x_k$  is mapped or encoded into the bit-string  $x'_m$  using the specific SBC coding scheme employed. Subsequently the output bit-string after SBC coding is interleaved using the bit-interleaver II of Figure 1, yielding the interleaved sequence  $\bar{x}_m$ , which is then encoded by a RSC code having a specific code rate given in Table I. Interleaving and de-interleaving constitute an important step in the iterative decoder of Figure 1, ensuring that the bits are input in their expected original order to the component decoders and ascertaining that the statistical independence of the extrinsic Log-Likelihood-Ratios (LLRs) is retained. Since in addition to the specific design of the interleaver the degree of statistical independence guaranteed by an interleaver is also related to its length [34], instead of performing the ISCD operation on the various frame slices independently, we

<sup>2</sup>The superscript \* was adopted from [27]

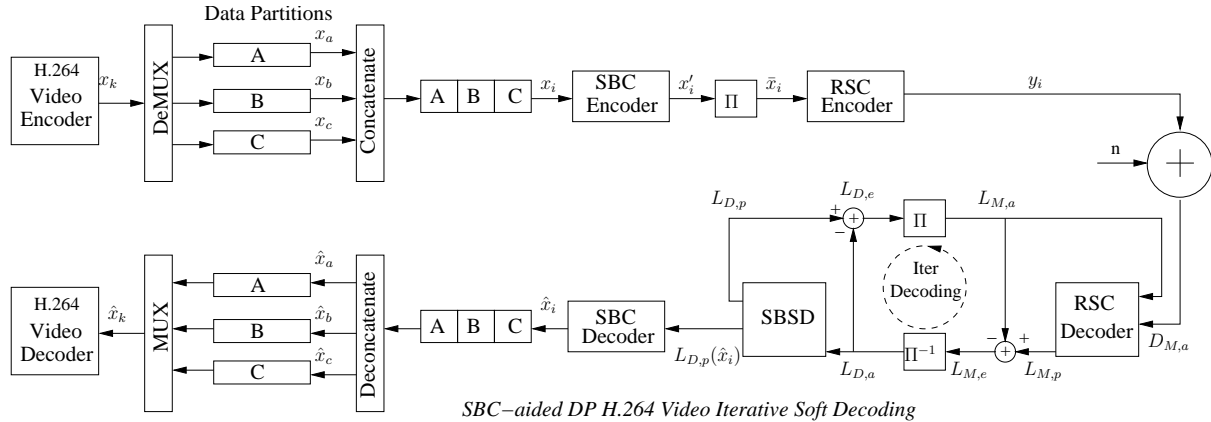


Fig. 1. The proposed system model

concatenated all the bits generated by each type of partition for the different Macro Blocks (MBs) within each slice of a given frame, which results in a longer interleaver without extending the video delay and hence improves the achievable performance of iterative decoding. The resultant bit-stream is QPSK modulated and transmitted over a temporally correlated narrowband Rayleigh fading channel, associated with the normalised Doppler frequency of  $f_d = f_D T_s = 0.01$ , where  $f_D$  is the Doppler frequency and  $T_s$  is the symbol duration. At the receiver the signal is QPSK demodulated and the resultant soft-information is passed to the RSC decoder. The extracted extrinsic information is then exchanged between the SBSD and RSC decoders of Figure 1 [11]. Following QPSK demodulation at the receiver the soft information is extracted in the form of its Log-Likelihood Ratio (LLR) representation  $D_{M,a}$ . This soft-information  $D_{M,a}$  is forwarded to the RSC inner decoder, which processes it along with the *a priori* information  $L_{M,a}$  fed back from the outer decoder of Figure 1 in order to generate the *a posteriori* LLR values  $L_{M,p}$ . The *a priori* LLR values  $L_{M,a}$  fed back from the outer decoder are subtracted from the inner decoder's output *a posteriori* LLR values  $L_{M,p}$  to generate the extrinsic LLR values  $L_{M,e}$ , which are subsequently deinterleaved by the soft-bit interleaver of Figure 1, yielding the soft-bits  $L_{D,a}$  that are input to the outer decoder to compute the *a posteriori* LLR value  $L_{D,p}$ . Observe in Figure 1 that  $L_{D,e}$  is generated by subtracting the *a priori* information  $L_{D,a}$  from the *a posteriori* information  $L_{D,p}$ , which in turn results in  $L_{M,a}$  after interleaving. During iterative decoding the outer decoder exploits the input LLR values for the sake of providing improved *a priori* information for the inner channel decoder of Figure 1, which in turn exploits the fed back *a priori* information in the subsequent iteration for the sake of providing improved *a posteriori* LLR values for the outer decoder. Further details about iterative decoding are provided in [35].

### C. Soft Bit Source Decoding

The conventional SBSD scheme gleans its extrinsic information from the natural residual redundancy, which inherently remains in the bit-stream after source encoding and manifests itself in terms of the non-uniform probability of occurrence of the resultant bit-patterns. More explicitly, for SBC coding the

source-encoded bit-stream is partitioned into  $M = 2^K$ -ary, or  $K$ -bit symbols, each of which has a different probability of occurrence and will be termed as the information word encoded by the proposed SBC. The redundancy of the source bit-stream is then characterised with the aid of the non-uniform  $M = 2^K$ -ary symbol probability distribution  $P[S_K(\tau)]$ , where  $S_K(\tau) = [S_K(1), S_K(2), \dots, S_K(M)]$ , with  $K$  denoting the number of bits in each  $M = 2^K$ -ary symbol<sup>3</sup>. The details regarding extrinsic information generation algorithm using SBSD for the zero-order Markov model can be obtained from [11]. Provided that the bits of an  $M = 2^K$ -ary symbol may be considered independent of each other, the channels' output information generated for the  $\tau$ -th  $K$ -bit symbol is generated by the product of each of the constituent single-bit probabilities given as:

$$P[\hat{y}_\tau | y_\tau] = \prod_{k=1}^K P[\hat{y}_\tau(k) | y_\tau(k)], \quad (1)$$

where  $\hat{y}_\tau = [\hat{y}_\tau(1), \hat{y}_\tau(2) \dots \hat{y}_\tau(K)]$ , is the received  $K$ -bit SBC coded sequence representing the  $\tau$ -th  $M$ -ary symbol, while  $y_\tau = [y_\tau(1), y_\tau(2) \dots y_\tau(K)]$  is the corresponding transmitted bit-sequence, again, provided that all these bits are independent of each other. For each desired bit  $[y_\tau(\lambda)]$ , the extrinsic channel output information  $P[\hat{y}_\tau^{[ext]} | y_\tau^{[ext]}]$  is expressed as:

$$P[\hat{y}_\tau^{[ext]} | y_\tau^{[ext]}] = \prod_{\substack{k=1, k \neq \lambda}}^K P[\hat{y}_\tau(k) | y_\tau(k)]. \quad (2)$$

Finally, the resultant extrinsic LLR value can be acquired for each bit of the  $\tau$ -th symbol by combining its channel output information and the *a-priori* knowledge of the corresponding  $\tau$ -th symbol as [9, 11]:

$$L[y_\tau(\lambda)] = \log \left( \frac{\sum_{y_\tau^{[ext]}} P[y_\tau^{[ext]} | y_\tau(\lambda) = +1] \cdot P[\hat{y}_\tau^{[ext]} | y_\tau^{[ext]}]}{\sum_{y_\tau^{[ext]}} P[y_\tau^{[ext]} | y_\tau(\lambda) = -1] \cdot P[\hat{y}_\tau^{[ext]} | y_\tau^{[ext]}]} \right). \quad (3)$$

<sup>3</sup>The choice of how many bits are specifically grouped into an  $M = 2^K$ -ary symbol represents an important system parameter, but due to space limitations this issue is not detailed in this paper.

TABLE I  
DIFFERENT SBCs WITH CORRESPONDING SYMBOLS, MINIMUM HAMMING DISTANCES ( $d_{H,min}$ ) AND CODE RATES.

SBC Type		Symbols in Decimal	$d_{H,min}$	Code Rate		
	Rate-1 SBC	{0,1}	1	RSC	SBC	Overall
				1/4	1	1/4
Algorithm-I	Rate- $\frac{2}{3}$ SBC $_{[2, 3]}$	{0,3,5,6}	2	3/8	2/3	1/4
	Rate- $\frac{3}{4}$ SBC $_{[3, 4]}$	{0,3,5,6,9,10,12,15}	2	1/3	3/4	1/4
	Rate- $\frac{4}{5}$ SBC $_{[4, 5]}$	{0,3,5,6,9,10,12,15,17,18,20,23,24,27,29,30}	2	5/16	4/5	1/4
	Rate- $\frac{5}{6}$ SBC $_{[5, 6]}$	{0,3,5,6,9,10,12,15,17,18,20,23,24,27,29,30,33, 34,36,39,40,43,45,46,48,51,53,54,57,58,60,63}	2	3/10	5/6	1/4
Algorithm-II	Rate- $\frac{1}{3}$ SBC $_{[2, 6]}$	{0,22,41,63}	3	3/4	1/3	1/4
	Rate- $\frac{1}{3}$ SBC $_{[3, 9]}$	{0,78,149,219,291,365,438,504}	4	3/4	1/3	1/4
	Rate- $\frac{1}{3}$ SBC $_{[4, 12]}$	{0,286,557,819,1099,1365,1638,1912,2183,2457, 2730,2996,3276,3538,3809,4095}	5	3/4	1/3	1/4
	Rate- $\frac{1}{3}$ SBC $_{[5, 15]}$	{0,1086,2141,3171,4251,5285,6342,7416,8471,9513, 10570,11636,12684,13746,14801,15855,16911,17969, 19026,20076,21140,22186,23241,24311,25368,26406, 27461,28539,29571,30653,31710,32736}	6	3/4	1/3	1/4
Algorithm-I	Rate-1 SBC	{0,1}	1	1/2	1	1/2
	Rate- $\frac{2}{3}$ SBC $_{[2, 3]}$	{0,3,5,6}	2	3/4	2/3	1/2

Although the proposed technique is generic and hence it is applicable to arbitrary speech, audio and video source codecs, in our design example the source coded bit-stream's redundancy is characterised with the aid of the non-uniform  $M$ -ary symbol probability distribution<sup>3</sup> using the H.264/AVC video encoded bit-stream of the 300 frame "Akiyo" video sequence, the 150 frame "MissAmerica" video clip and the 300-frame "Mother&Daughter" video sequence, which were used as training sequences.

### III. SHORT BLOCK CODE BASED ITERATIVE SOURCE CHANNEL DECODING

#### A. Iterative Convergence

The purpose of ISCD is to utilise the constituent inner and outer decoders in order to assist each other in an iterative fashion to glean the highest possible extrinsic information ( $L_{SBS}^{extr}(x')$  and  $L_{RSC}^{extr}(\bar{x})$ ) from each other. In fact, the achievable performance of SBSD is limited by the factor that its achievable iteration gain is actually dependent on the residual redundancy or correlation that remains in the coded bit pattern  $x_i$  after limited-complexity, limited-delay, lossy source encoding [1]. However, despite using limited-complexity, limited-delay, lossy compression, the achievable performance improvements of SBSD may remain limited due to the limited residual redundancy in the video-encoded bit-stream, when using the high-compression H.264/AVC video codec. It may be observed from the simulation results of [36] that typically using SBSD for H.264/AVC coded bit-stream results in negligible system performance improvements beyond two decoding iterations. Hence, in order to improve the

<sup>3</sup>The resultant  $M$ -ary source word probability distribution for the SBC $_{[K,N]}$  coding schemes used in our design example is not provided in this paper owing to space limitations.

achievable ISCD performance gain, we *artificially* introduce redundancy in the source coded bit-stream using a technique which we refer to as SBC coding. The novel philosophy of our SBC design is based on exploiting a specific property of Extrinsic Information Transfer (EXIT) Charts [37]. More explicitly, an iterative decoding aided receiver is capable of near-capacity operation at an infinitesimally low decoded BER, if there is an open tunnel between the EXIT curves of the inner and outer decoder components. We will demonstrate that this condition is clearly satisfied, when these two EXIT curves have a point of intersection at the  $(I_A, I_B) = (1, 1)$  corner of the EXIT chart, where  $I_A = I(x'_i, L_{D,a})$ ,  $0 \leq I_A \leq 1$  bit, is the mutual information between the outer encoded bits  $x'_i$  and the LLR values  $L_{D,a}$ , while  $I_E = I(x'_i, L_{D,e})$ ,  $0 \leq I_E \leq 1$  bit, represents the mutual information between the outer channel coded bits  $x'_i$  and the LLR values  $L_{D,e}$ . The *sufficient and necessary* condition for this iterative detection convergence criterion to be met in the presence of perfect *a priori* information, was shown in detail by Kliewer *et al.* [38] to be that the legitimate codewords have a minimum Hamming distance of  $d_{H,min} = 2$ . Then the ISCD scheme becomes capable of achieving the highest possible source entropy denoted as  $H(X) = 1$  bit, provided that the input *a priori* information of the SBSD is perfect. This motivates the design of the proposed SBC schemes, because it is plausible that using our design procedure all legitimate SBC codewords having a specific mapping-rate equivalent to the reciprocal of the classic code-rate results in a code-table satisfying the condition of  $d_{H,min} \geq 2$ . Using appropriately designed SBCs it may be guaranteed that the EXIT curve of the combined source codec and SBC block becomes capable of reaching the  $(I_A, I_E) = (1, 1)$  point of perfect convergence i.e. the

maximum  $I_E$  will be taken at the  $I_A = 1$  point of the EXIT chart [11], regardless of the EXIT-curve shape of the stand-alone source encoder.

Having outlined the theoretical justification for achieving perfect convergence to an infinitesimally low BER, let us now introduce the proposed SBC<sub>[K, N]</sub> encoding algorithms, which maps or encodes each  $K$ -bit symbol of the source set  $X$  to the  $N$ -bit code words of the SBC set  $f(X)$ , while maintaining a minimum Hamming distance of  $d_{H,min} \geq 2$ . According to our SBC<sub>[K, N]</sub> encoding procedure, the video-stream  $x_k$  is partitioned into  $M = 2^K$ -ary, or  $K$ -bit source symbols, each of which has a different probability of occurrence and will be alternatively termed as the information word to be encoded into  $N = (K + P)$ -bits, where  $P$  represents the number of redundant bits per  $K$ -bit source symbol.

#### Algorithm-I:

For  $P = 1$ , the redundant bit  $r_\tau$  is generated for the  $\tau$ -th  $M$ -ary source symbol by calculating the *exclusive OR* (*XOR*) function of its  $K$  constituent bits, as follows:

$$r_\tau = [b^\tau(1) \oplus b^\tau(2) \dots \oplus b^\tau(K)], \quad (4)$$

where  $\oplus$  represents the *XOR* operation.

The resultant redundant bit can be incorporated in any of the  $[K + 1]$  different bit positions, in order to create  $[K + 1]$  different legitimate SBC-encoded words, as presented in Table II, each having a minimum Hamming distance of  $d_{H,min} = 2$  from all the others. The encoded symbols of the rate- $\frac{2}{3}$ ,  $\frac{3}{4}$ ,  $\frac{4}{5}$  and  $\frac{5}{6}$  SBCs along with their corresponding minimum Hamming distance  $d_{H,min}$  is summarised in Table I for the specific case of incorporating the redundant bit  $r_\tau$  at the end of the  $\tau$ -th  $K$ -bit source symbol.

#### Algorithm-II:

For  $P = (m \times K)$  with  $m \geq 1$ , we propose the corresponding SBC<sub>[K, N]</sub>-encoding procedure, which results in a gradual increase of  $d_{H,min}$  for the coded symbols upon increasing both  $K$  and  $N$  of the SBC<sub>[K, N]</sub>, while the code-rate is fixed. This  $K$  to  $N$ -bit encoding method consists of two steps,

##### 1) STEP-1:

First  $R_b = [(m - 1) \times K]$  number of redundant bits  $r_\tau(r)$ , for  $r = 1, 2 \dots R_b$  are concatenated to the  $\tau$ -th  $K$ -bit source symbol by repeated concatenation of  $K$  additional source coded bits  $(m - 1)$  times, yielding a total of  $[(m - 1) \times K]$  bits, as shown in Table III.

##### 2) STEP-2:

In the Second step the last set of  $K$  redundant bits  $r_\tau(k)$ , for  $k = 1, 2 \dots K$  is generated by calculating the *XOR* function of the  $K$  source bits  $b_\tau(j)$ , while setting  $b_\tau[j = k]$  equal to 0, yielding:

$$r_\tau(k) = [b_\tau(1) \oplus b_\tau(2) \dots \oplus b_\tau(K)];$$

for  $k = 1, 2 \dots K$ , while setting  $b_\tau(k) = 0$ , as presented in Table III, where  $\oplus$  represents the *XOR* operation.

Using this method a carefully controlled redundancy is imposed by the specific rate  $r = [\frac{K}{N}]$  SBC<sub>[K, N]</sub> to ensure that the resultant  $N$ -bit codewords exhibit a minimum Hamming

distance of  $d_{H,min} \geq 2$  between the  $M = 2^K$  number of legitimate  $K$ -bit source code words. This method also results in a gradual increase of the  $d_{H,min}$  of the coded symbols upon increasing both  $K$  and  $N$  of the SBC<sub>[K, N]</sub> considered, as shown in Table I, until the maximum achievable  $d_{H,min}$  is reached for the specific SBC coding rate.

TABLE II  
SBC CODING PROCEDURE USING ALGORITHM-I.

INPUT	OUTPUT COMBINATIONS			
	C <sub>1</sub>	C <sub>2</sub>	...	C <sub>K+1</sub>
S <sub>(1)</sub>	$r_1 x_1 x_2 \dots x_K$	$x_1 r_1 x_2 \dots x_K$	.	$x_1 x_2 \dots x_K r_1$
S <sub>(2)</sub>	$r_2 x_1 x_2 \dots x_K$	$x_1 r_2 x_2 \dots x_K$	.	$x_1 x_2 \dots x_K r_2$
:	:	:	:	:
S <sub>(2K)</sub>	$r_{2K} x_1 x_2 \dots x_K$	$x_1 r_{2K} x_2 \dots x_K$	.	$x_1 x_2 \dots x_K r_{2K}$

#### B. Design Example

Let us now demonstrate the power of SBCs with the aid of a design example. As an example, the SBC<sub>[K, N]</sub>-encoded symbols generated by applying rate- $\frac{2}{3}$ ,  $\frac{3}{4}$ ,  $\frac{4}{5}$ ,  $\frac{5}{6}$  and rate- $\frac{1}{3}$  coding schemes generated using Algorithm-I and Algorithm-II are detailed in Table I, along with their corresponding minimum Hamming distances  $d_{H,min}$ . Again, as it becomes evident from Table I, the EXIT-chart optimised SBCs ensure that the encoded  $N$ -bit symbols exhibit a minimum Hamming distance of  $d_{H,min} \geq 2$ . Additionally, only  $2^K$  out of the  $2^N$  possible  $N$ -bit symbols are legitimate in the mapped source coded bit-stream, which exhibits a non-uniform probability of occurrence for the  $N$ -bit source symbols. Figure 2 depicts the EXIT characteristics of the SBS<sub>D</sub> scheme of Figure 1 using either the rate- $\frac{1}{4}$  or the rate- $< 1$  SBC<sub>[K, N]</sub> schemes of Algorithm-I and II shown in Table I. More specifically, the EXIT curve of SBS<sub>D</sub> using rate- $\frac{1}{3}$ ,  $\frac{2}{3}$ ,  $\frac{3}{4}$ ,  $\frac{4}{5}$  and  $\frac{5}{6}$  SBCs does indeed reach to the top right corner of the EXIT chart at  $(I_A, I_E) = (1, 1)$  and hence results in an infinitesimally low BER. By contrast, the SBS<sub>D</sub> scheme using a rate-1 SBC, i.e. no SBC fails to do so. In conclusion, our simulation results recorded for the system presented in Figure 1 reveal that the performance of SBS<sub>D</sub> strongly depends on the presence or absence of residual source redundancy, which typically manifests itself in the form of non-uniform probability of occurrence for the  $N$ -bit source coded symbols. The coding parameters of the different SBC schemes used in our design example are shown in Table I. In this design example our primary aim is to analyse the performance of the proposed Algorithm-I and II in conjunction with various SBCs having different coding rates and  $d_{H,min}$ . For this reason we selected rate- $\frac{1}{3}$  SBCs generated using Algorithm-II, which provide sufficiently diverse  $d_{H,min}$  values of 3, 4, 5 and 6 in order to analyse the associated effects on the achievable performance, while employing an RSC code as our inner code. Therefore, considering a rate- $\frac{1}{3}$  SBC code along with a rate- $\frac{3}{4}$  inner RSC code resulted in an overall system code rate of  $\frac{1}{4}$ . We considered a concatenated

<sup>4</sup>For the sake of using a unified terminology, we refer to the scheme using no SBC as the rate-1 SBC.

TABLE III  
SBC CODING PROCEDURE USING ALGORITHM-II.

INPUT	$x_1 x_2 \dots x_K$				
STEPS	STEP-1				STEP-2
Repeated $K$ -bit Concatenation	$1^{st}$	$2^{nd}$	$\dots$	$(m+1)^{th}$	$m^{th}$
OUTPUT	$x_1 x_2 \dots x_K$	$x_1 x_2 \dots x_K$	$\dots$	$x_1 x_2 \dots x_K$	$x'_1 x'_2 \dots x'_K$
where, $x'_1 = (0 \oplus x_2 \oplus \dots \oplus x_K)$ , $x'_2 = (x_1 \oplus 0 \oplus \dots \oplus x_K)$ , $\dots$ , $x'_K = (x_1 \oplus x_2 \oplus \dots \oplus 0)$					

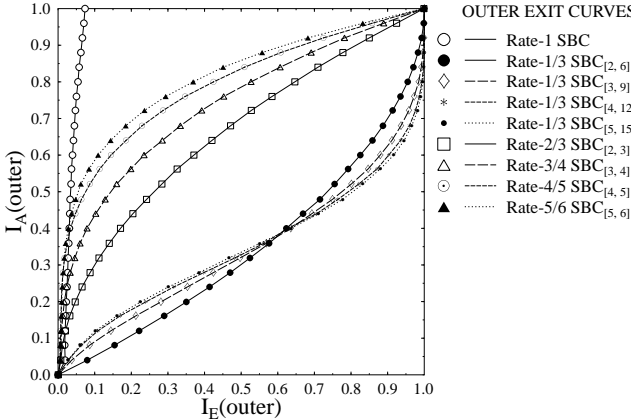


Fig. 2. EXIT characteristics of SBSD with the aid of different SBCs.

rate  $R = \frac{1}{4}$  RSC encoder with constraint length  $L = 4$  and generator sequences  $g_1 = [1011]$ ,  $g_2 = [1101]$ ,  $g_3 = [1101]$  and  $g_4 = [1111]$  represented as  $G = [1, g_2/g_1, g_3/g_1, g_4/g_1]$ , where '1' denotes the systematic output, the first output  $g_1$  is fed back to the input and  $g_2, g_3, g_4$  denotes the feed forward output of the RSC encoder. Additionally, for the SBC performance evaluation using our proposed system with relatively high overall system code-rate of  $R = \frac{1}{2}$  presented in Table I, we utilised a concatenated rate  $R = \frac{1}{2}$  RSC encoder with constraint length  $L = 3$  and generator sequences  $g_1 = [111]$  and  $g_2 = [101]$  represented as  $G = [1, g_2/g_1]$ . Observe from the table that an overall code-rate of  $R = \frac{1}{4}$  and  $R = \frac{1}{2}$  was maintained by adjusting the puncturing rate of the concatenated RSC in order to accommodate the different SBC rates of Table I.

#### IV. EXIT CHART ANALYSIS

At the receiver seen in Figure 1, iterative soft-bit source and channel decoding is applied by exchanging extrinsic information between the receiver blocks, which has the capability of improving the achievable subjective video quality. EXIT charts were utilised to characterize the mutual information exchange between the input and output of both the inner and outer components of an iterative decoder and hence to analyse its decoding convergence behaviour. Additionally, the actual decoding trajectories acquired while using various SBCs generated using Algorithm-I and II were presented by recording the mutual information at the input and output of both the inner and outer decoder during the bit-by-bit Monte-Carlo simulation of the iterative SBSD algorithm.

Figures 3 present the decoding trajectories recorded at  $E_b/N_0 = 0 \text{ dB}$  and  $-1 \text{ dB}$ , when employing the rate- $\frac{2}{3}$  SBCs of Algorithm-I as the outer code along with the corresponding rate- $\frac{3}{4}$  RSC code.

Furthermore, the decoding trajectories obtained by employing rate- $\frac{1}{3}$  outer SBCs of type SBC $_{[5, 15]}$ , which were generated using Algorithm-II as well as using the rate- $\frac{3}{4}$  inner RSC detailed in Table I was recorded at  $E_b/N_0 = -4 \text{ dB}$  and  $-4.5 \text{ dB}$ , as portrayed in Figures 4. It may be observed from the EXIT trajectories of Figures 3, and 4 that as expected, the convergence behaviour of SBCs improves upon increasing  $d_{H,min}$ .

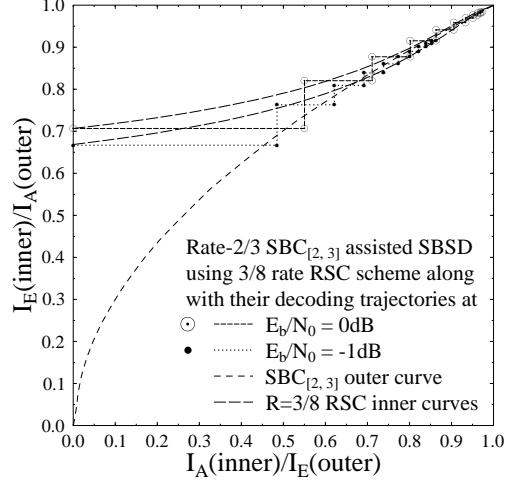


Fig. 3. The EXIT chart and simulated decoding trajectories of the SBC $_{[2, 3]}$  scheme at  $E_b/N_0 = 0$  and  $-1 \text{ dB}$ .

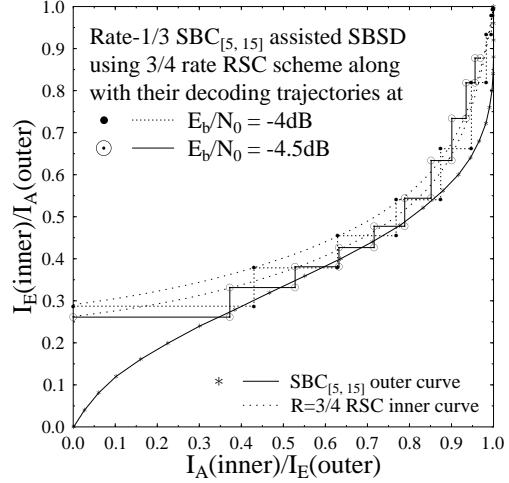


Fig. 4. The EXIT chart and simulated decoding trajectories of the SBC $_{[5, 15]}$  scheme at  $E_b/N_0 = -4$  and  $-4.5 \text{ dB}$ .

#### V. SYSTEM PERFORMANCE RESULTS

In this section we present our performance results for the proposed system. A 45 frame "Akiyo" video sequence [1] in (176x144)-pixel Quarter Common Intermediate Format (QCIF) was used as our test sequence and was encoded

using the H.264/AVC JM 13.2 reference video codec at 15 frames-per-second (*fps*) at the target bitrate of 64 *kbps*. Using H.264/AVC codec each QCIF frame was partitioned into 9 slices and each slice was composed of 11 MBs. The resultant video encoded clip consisted of an intra-coded 'I' frame followed by 44 predicted or 'P' frames, corresponding to a lag of 3 seconds between the 'I' frames at a frame-rate of 15 *fps*. The periodic insertion of 'T' frames curtailed error propagation beyond 45 frames.

Additional source codec parameters were set as follows,

- quarter-pixel motion estimation resolution was used;
- intra frame MB update was used;
- all macroblock types were enabled;
- no multiframe prediction was used;
- no B-slices were used;
- Universal Variable Length Coding (UVLC) type entropy coding was used;
- error concealment was performed using the motion vector recovery algorithm of [39];

To control the effects of error propagation, we incorporated error resilience features, such as DP and intra-frame coded MB updates of three randomly distributed MBs per frame. The insertion of 'B' pictures was avoided because it results in an unacceptable loss of lip-synchronisation as a result of the corresponding delay incurred due to the bi-directionally predicted video coding operations [39]. Additionally, only the immediately preceding frame was used for motion search, which results in a reduced computational complexity compared to using multiple reference frames. These video coding parameters were chosen, bearing in mind that the error-resilience of the DP aided H.264/AVC stream is directly related to the number of 'P' frames inserted between two consecutive 'I' frames.

The remaining error resilient encoding techniques, such as the employment of multiple reference frames for inter-frame motion compensation and Flexible Macro-block Ordering (FMO) [40] were turned off, because they typically result in modest video performance improvements in low-motion head-and-shoulders video sequences, such as the "Akiyo" clip, despite their substantially increased complexity. These encoder settings result in a reduced encoder complexity and in a realistic real-time implementation. Moreover, since handheld videophones have to have a low complexity, we limited the number of iterations between the RSC and SBSD decoders to  $I_t = 10$ , when using a rate-1 SBC – i.e. no SBC. Similarly, we used  $I_t = 10$  iterations, when applying SBCs having a rate below unity. For the sake of increasing the confidence in our results, we repeated each 45-frame experiment 160 times and averaged the results generated. A range of different SBCs generated using our proposed *Algorithm-I* and *II* are given in Table I, which are used as the outer codes of Figure 1 in order to evaluate their achievable system performance improvements. We evaluated the performance of our proposed system by keeping the same overall code rate as well as video rate for the different considered error protection schemes.

Figure 5 presents the performance of the various rate- $\frac{2}{3}$ ,

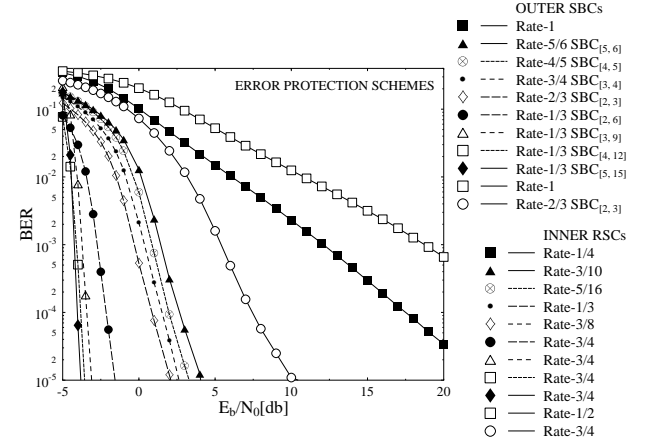


Fig. 5. BER vs  $E_b/N_0$  performance of the various error protection schemes summarised in Table I.

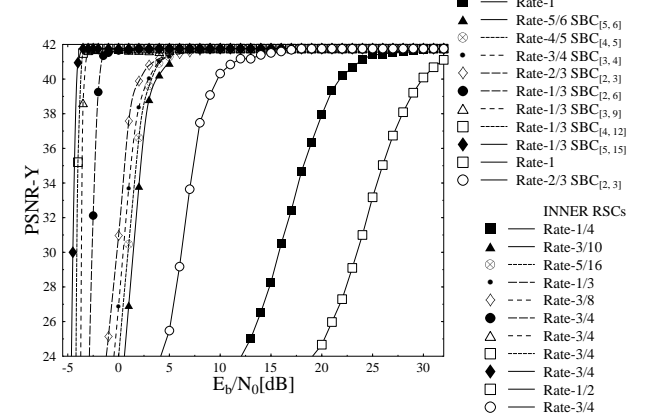


Fig. 6. PSNR-Y vs  $E_b/N_0$  performance of various error protection schemes summarised in Table I.

$\frac{3}{4}$ ,  $\frac{4}{5}$  and  $\frac{5}{6}$  SBCs along with the rate- $\frac{1}{3}$  SBC based error protection schemes of Table I in terms of the attainable BER in comparison with the rate-1 SBC based scheme. Additionally, the performance trends expressed in terms of the *PSNR* versus  $E_b/N_0$  curves are portrayed in Figures 6. It may be observed in Figure 6 that the SBC $_{[5, 15]}$  scheme having  $d_{H, \min} = 6$  provides the best PSNR performance among the eight different SBC schemes of Table I across the entire  $E_b/N_0$  region considered. Furthermore, observe from Figure 6 that the lowest rate- $\frac{2}{3}$  outer SBC combined with rate- $\frac{3}{8}$  inner RSC results in the best PSNR performance, outperforming the rate- $\frac{3}{4}$ ,  $\frac{4}{5}$  and  $\frac{5}{6}$  SBCs generated using Algorithm-I. It may also be observed in Figure 6 that using SBSD in conjunction with the rate-1 outer SBC and rate- $\frac{1}{4}$  inner RSC results in a worse PSNR performance than the outer SBCs having a less than unity rate combined with the corresponding inner RSC of Table I, while maintaining the same overall code rate. Additionally, Figure 5 and Figure 6 also presents the BER and PSNR performance of our proposed system while employing rate- $\frac{2}{3}$  SBCs relative to rate-1 SBC based scheme, while considering an overall system code rate of  $R = \frac{1}{2}$ . Quantitatively, using the SBCs of Table I having a rate lower than 1 and overall system code rate of  $R = \frac{1}{4}$ , an additional  $E_b/N_0$  gain of upto 25 dB may be achieved over the rate-1 SBC at the PSNR degradation point of 1 dB.

Finally, the achievable subjective video qualities of the

video telephone schemes utilising various types of SBCs generated using *Algorithm-I* and *II* is presented in Figures 7 and 8, respectively. In order to have a fair subjective video quality comparison, we averaged both the luminance and chrominance components of the 30 video test sequences, decoded using the H.264 video codec for each type of setup. The achievable subjective video quality recorded at the channel  $E_b/N_0$  value of 0.5 dB using rate- $\frac{2}{3}$ ,  $\frac{3}{4}$ ,  $\frac{4}{5}$ , and  $\frac{5}{6}$  SBCs of *Algorithm - I* can be seen in Figure 7. Observe from Figure 7 that the achievable video quality improves upon decreasing the SBC code rate.

Similarly, Figure 8 presents the subjective video quality obtained at (from left to right)  $E_b/N_0 = -4.1$  dB,  $-3.9$  dB,  $-3.0$  dB and  $-2.1$  dB using rate- $\frac{1}{3}$  SBCs of the type (from top to bottom) SBC<sub>[2, 6]</sub>, SBC<sub>[3, 9]</sub>, SBC<sub>[4, 12]</sub> and SBC<sub>[5, 15]</sub>. Observed from Figure 8 that a nearly unimpaired quality is obtained for the rate- $\frac{1}{3}$  SBCs having (from top)  $d_{H,min} = 3, 4, 5$  and  $6$  at  $E_b/N_0$  values of  $-2.5$  dB,  $-3.0$  dB,  $-3.9$  dB and  $-4.1$  dB, respectively. This implies that the subjective video quality of the system improves upon increasing  $d_{H,min}$  of the SBCs employed.



Fig. 7. Subjective video quality of the 45<sup>th</sup> "Akiyo" video sequence frame using (from left) Rate- $\frac{2}{3}$ ,  $\frac{3}{4}$ ,  $\frac{4}{5}$  and  $\frac{5}{6}$  SBCs of Algorithm-I summarised in Table I at  $E_b/N_0 = 0.5$  dB.



Fig. 8. Subjective video quality of the 45<sup>th</sup> "Akiyo" video sequence frame using Rate- $\frac{1}{3}$  SBCs of type (from top) SBC<sub>[2, 6]</sub>, SBC<sub>[3, 9]</sub>, SBC<sub>[4, 12]</sub> and SBC<sub>[5, 15]</sub> of Algorithm-II summarised in Table I at (from left)  $E_b/N_0 = -4.1$  dB,  $-3.9$  dB,  $-3$  dB and  $-2.1$  dB.

## VI. CONCLUSIONS

In this paper we proposed generic low-complexity SBCs for satisfying the *necessary and sufficient* condition of  $d_{H,min} = 2$  and hence guaranteeing decoding convergence for arbitrary SBSD-aided multimedia source codecs. We applied diverse error protection schemes considering the transmission of DP aided H.264/AVC coded video using carefully selected SBCs

having diverse  $d_{H,min}$  values. Furthermore, iterative soft-bit source and channel decoding was used to enhance the attainable BER performance and to improve the objective video quality expressed in terms of PSNR. It was demonstrated that the bit-error correction capability of the ISCD scheme was significantly improved with the advent of rate- $\frac{1}{3}$  SBC scheme owing to the intentional increase in redundancy of the source coded bit-stream, when we beneficially partitioned the total available bit rate budget between the source and channel codecs. Additionally, the convergence behaviour of the ISCD system was analysed using EXIT charts. The H.264 / SBC / RSC design example using SBCs having  $d_{H,min} = 6$  exhibited an  $E_b/N_0$  gain of 2.25 dB at the *PSNR* degradation point of 1 dB over the identical-rate SBCs having  $d_{H,min} = 3$ . Additionally, an  $E_b/N_0$  gain of 9 dB was achieved compared to the rate- $\frac{5}{6}$  SBCs having  $d_{H,min} = 2$  and an identical overall code-rate. Moreover, an  $E_b/N_0$  gain of 25 dB was attained at the *PSNR* degradation point of 1 dB using iterative soft-bit source and channel decoding with the aid of rate- $\frac{1}{3}$  SBCs in comparison to the identical-rate benchmark. Our future research will consider the design of systematic variable-length SBC coding techniques to intentionally introduce redundancy in the source coded bit-stream based on the relative importance of the different H.264/AVC partitions.

## REFERENCES

- [1] L. Hanzo, P. Cherriman, and J. Streit, *Video Compression and Communications: From Basics to H.261, H.263, H.264, MPEG2, MPEG4 for DVB and HSDPA-Style Adaptive Turbo-Transceivers*. Wiley-IEEE Press, 2007.
- [2] L. Hanzo, C. Somerville, and J. Woodard, *Voice and Audio Compression for Wireless Communications*, 2nd Edition. Wiley-IEEE Press, 2007.
- [3] R. Stedman, H. Gharavi, L. Hanzo, and R. Steele, "Transmission of subband-coded images via mobile channels," *IEEE Transactions on Circuits and Systems for Video Technology*, vol. 3, pp. 15–26, Feb. 1993.
- [4] L. Hanzo and J. Streit, "Adaptive low-rate wireless videophone schemes," *IEEE Transactions on Circuits and Systems for Video Technology*, vol. 5, pp. 305–318, Aug. 1995.
- [5] J. Streit and L. Hanzo, "Dual-mode vector-quantized low-rate cordless videophone systems for indoors and outdoors applications," *IEEE Transactions on Vehicular Technology*, vol. 46, pp. 340–357, May 1997.
- [6] J. Streit and L. Hanzo, "Quadtree-based reconfigurable cordless videophone systems," *IEEE Transactions on Circuits and Systems for Video Technology*, vol. 6, pp. 225–237, Apr. 1996.
- [7] L. Hanzo, P. Cherriman, and E. L. Kuan, "Interactive cellular and cordless video telephony: State-of-the-art system design principles and expected performance," *Proceedings of the IEEE*, vol. 88, pp. 1388–1413, Sept. 2000.
- [8] S. X. Ng, J. Y. Chung, and L. Hanzo, "Turbo-detected unequal protection MPEG-4 wireless video telephony using multi-level coding, trellis coded modulation and space-time trellis coding," in *Communications, IEE Proceedings-*, vol. 152, pp. 1116–1124, Dec. 2005.
- [9] T. Fingscheidt and P. Vary, "Softbit speech decoding: a new approach to error concealment," *IEEE Transactions on Speech and Audio Processing*, vol. 9, pp. 240–251, Mar. 2001.
- [10] T. Fingscheidt, S. Heinén, and P. Vary, "Joint speech codec parameter and channel decoding of parameterindividual block codes (PIBC)," in *Speech Coding Proceedings, 1999 IEEE Workshop on*, (Porvoo, Finland), pp. 75–77, 1999.
- [11] M. Adrat and P. Vary, "Iterative source-channel decoding: improved system design using exit charts," *EURASIP J. Appl. Signal Process.*, vol. 2005, no. 1, pp. 928–941, 2005.
- [12] R. Perkert, M. Kaindl, and T. Hindelang, "Iterative source and channel decoding for GSM," in *Acoustics, Speech, and Signal Processing, 2001. Proceedings. (ICASSP '01). 2001 IEEE International Conference on*, vol. 4, (Salt Lake City, UT, USA), pp. 2649–2652, 2001.

- [13] J. Ostermann, J. Bormans, P. List, D. Marpe, M. Narroschke, F. Pereira, T. Stockhammer, and T. Wedi, "Video coding with H.264/AVC: tools, performance, and complexity," *IEEE Circuits and Systems Magazine*, vol. 4, no. 1, pp. 7–28, 2004.
- [14] A. Guyader, E. Fabre, C. Guillemot, and M. Robert, "Joint source-channel turbo decoding of entropy-coded sources," *IEEE Journal on Selected Areas in Communications*, vol. 19, pp. 1680–1696, Sept. 2001.
- [15] J. Kliewer and R. Thobaben, "Iterative joint source-channel decoding of variable-length codes using residual source redundancy," *IEEE Transactions on Wireless Communications*, vol. 4, pp. 919–929, May 2005.
- [16] J. Liu, G. Tu, C. Zhang, and Y. Yang, "Joint source and channel decoding for variable length encoded turbo codes," *EURASIP J. Adv. Signal Process*, vol. 2008, no. 1, pp. 1–10, 2008.
- [17] R. G. Maunder, J. Wang, S. X. Ng, L. L. Yang, and L. Hanzo, "On the performance and complexity of irregular variable length codes for near-capacity joint source and channel coding," *IEEE Transactions on Wireless Communications*, vol. 7, pp. 1338–1347, Apr. 2008.
- [18] L. Hanzo, P. Cherriman, and E. L. Kuan, "Interactive cellular and cordless video telephony: State-of-the-art system design principles and expected performance," *Proceedings of the IEEE*, vol. 88, pp. 1388–1413, Sept. 2000.
- [19] L. Hanzo, B. Jonathan, and N. Song, *3G, HSPA and FDD versus TDD Networking: Smart Antennas and Adaptive Modulation*, 2nd Edition. Wiley-IEEE Press, February 2008.
- [20] L. Hanzo, T. H. Liew, and B. L. Yeap, *Turbo Coding, Turbo Equalisation and Space-Time Coding for Transmission over Fading Channels*. New York, NY, USA: John Wiley & Sons, 2002.
- [21] A. Q. Pham, J. Wang, L. L. Yang, and L. Hanzo, "An iterative detection aided irregular convolutional coded wavelet videophone scheme using reversible variable-length codes and map equalization," in *VTC2007-Spring. IEEE 65th*, (Dublin), pp. 2404–2408, Apr. 2007.
- [22] Nasruminallah, M. El-Hajjar, N. Othman, A. Quang, and L. Hanzo, "Over-complete mapping aided, soft-bit assisted iterative unequal error protection h.264 joint source and channel decoding," in *IEEE VTC'08 (Fall)*, p. 5 pages, September 2008.
- [23] Y. Wang and S. Yu, "Joint source-channel decoding for H.264 coded video stream," *IEEE Transactions on Consumer Electronics*, vol. 51, pp. 1273–1276, Nov. 2005.
- [24] T. Clevorn, P. Vary, and M. Adrat, "Iterative Source-channel Decoding Using Short Block Codes," in *Acoustics, Speech and Signal Processing, 2006. ICASSP 2006 Proceedings. 2006 IEEE International Conference on*, vol. 4, May 2006.
- [25] R. Thobaben, "A new transmitter concept for iteratively-decoded source-channel coding schemes," in *Signal Processing Advances in Wireless Communications, 2007. SPAWC 2007. IEEE 8th Workshop on*, pp. 1–5, June 2007.
- [26] R. Thobaben, L. Schmalen, and P. Vary, "Joint source-channel coding with inner irregular codes," in *Information Theory, 2008. ISIT 2008. IEEE International Symposium on*, pp. 1153–1157, July 2008.
- [27] M. Adrat, P. Vary, and T. Clevorn, "Optimized bit rate allocation for iterative source-channel decoding and its extension towards multi-mode transmission," in *Proceedings of IST Mobile and Wireless Communications Summit (Dresden, Germany)*, pp. 1153–1157, June 2005.
- [28] T. Clevorn, J. Brauers, M. Adrat, and P. Vary, "Turbo decodulation: iterative combined demodulation and source-channel decoding," *IEEE Communications Letters*, vol. 9, pp. 820–822, Sept. 2005.
- [29] T. Clevorn, J. Brauers, M. Adrat, and P. Vary, "EXIT chart analysis of turbo decodulation," in *Personal, Indoor and Mobile Radio Communications, 2005. PIMRC 2005. IEEE 16th International Symposium on*, vol. 2, pp. 711–715, Sept. 2005.
- [30] T. Clevorn, M. Adrat, and P. Vary, "Turbo decodulation using highly redundant index assignments and multi-dimensional mappings," *Proceedings of International Symposium on Turbo Codes & Related Topics*, Apr. 2006.
- [31] T. Clevorn, L. Schmalen, P. Vary, and M. Adrat, "On Redundant Index Assignments for Iterative Source-channel Decoding," *IEEE Communications Letters*, vol. 12, pp. 514–516, July 2008.
- [32] T. Wiegand, G. J. Sullivan, G. Bjntegaard, and A. Luthra, "Overview of the H.264/AVC video coding standard," *IEEE Transactions on Circuits and Systems for Video Technology*, vol. 13, pp. 560–576, July 2003.
- [33] ITU-T: H.264 Recommendation, "H.264 : Advanced video coding for generic audiovisual services," ([www.itu.int/rec/T-REC-H.264/en](http://www.itu.int/rec/T-REC-H.264/en)), p. 282, May 2003.
- [34] R. G. Maunder, J. Kliewer, S. X. Ng, J. Wang, L. L. Yang, and L. Hanzo, "Joint iterative decoding of trellis-based VQ and TCM," *IEEE Transactions on Wireless Communications*, vol. 6, pp. 1327–1336, Apr. 2007.
- [35] S. Benedetto, D. Divsalar, G. Montorsi, and F. Pollara, "Serial concatenation of interleaved codes: performance analysis, design and iterative decoding," *IEEE Transactions on Information Theory*, vol. 44, pp. 909–926, May 1998.
- [36] T. Hindelang, M. Adrat, T. Fingscheidt, and S. Heinen, "Joint source and channel coding: from the beginning until the 'EXIT,'" *European Transactions on Telecommunications*, vol. 18, no. 8, pp. 851–858, 2007.
- [37] S. ten Brink, "Designing iterative decoding schemes with the extrinsic information transfer chart," in *AEU International Journal of Electronics and Communications*, vol. 54, pp. 389–398, Nov. 2000.
- [38] J. Kliewer, N. Goertz, and A. Mertins, "Iterative source-channel decoding with markov random field source models," *IEEE Transactions on Signal Processing*, [see also *IEEE Transactions on Acoustics, Speech, and Signal Processing*], vol. 54, no. 10, pp. 3688–3701, Oct. 2006.
- [39] T. Stockhammer, M. M. Hannuksela, and T. Wiegand, "H.264/AVC in wireless environments," *IEEE Transactions on Circuits and Systems for Video Technology*, vol. 13, pp. 657–673, July 2003.
- [40] S. Wenger, "H.264/AVC over IP," *IEEE Transactions on Circuits and Systems for Video Technology*, vol. 13, pp. 645–656, July 2003.



**Nasruminallah** received the B.Sc. degree in computer engineering from University of Engineering & Technology (UET), Peshawar, Pakistan, in 2004 and the M.Sc. degree in computer engineering from Lahore University of Management Sciences (LUMS), Lahore, Pakistan, in 2006. Since March 2007, he has been working toward the Ph.D. degree at the Communications Group, School of Electronics and Computer Science, University of Southampton, Southampton, U.K. His research interests include low bit-rate video coding for wireless communications, turbo coding and detection, and iterative source-channel decoding.



**Lajos Hanzo**, Fellow of the Royal Academy of Engineering, received his first-class degree in electronics in 1976 and his doctorate in 1983. In 2004 he was awarded the Doctor of Sciences (DSc) degree by the University of Southampton, UK. During his career in telecommunications he has held various research and academic posts in Hungary, Germany and the UK. Since 1986 he has been with the Department of Electronics and Computer Science, University of Southampton, UK, where he holds the chair in telecommunications. He co-authored 15 John Wiley and IEEE Press books totalling 10 000 pages on mobile radio communications, published about 700 research papers, organised and chaired conference conferences, presented various keynote and overview lectures and has been awarded a number of distinctions. Currently he heads an academic research team, working on a range of research projects in the field of wireless multimedia communications sponsored by industry, the Engineering and Physical Sciences Research Council (EPSRC) UK, the European IST Programme and the Mobile Virtual Centre of Excellence (VCE), UK. He is an enthusiastic supporter of industrial and academic liaison and he offers a range of industrial courses. Lajos is also an IEEE Distinguished Lecturer of both the Communications as well as the Vehicular Technology Society, a Fellow of both the IEEE and the IEE. He is an editorial board member of the Proceedings of the IEEE and a Governor of the IEEE VT Society. For further information on research in progress and associated publications please refer to <http://www-mobile.ecs.soton.ac.uk>